Ecological scheme of cyanobacterial responses to hydrogen peroxide and antioxidant enzymes against diurnal light intensity

Takashi Asaeda (asaeda@mail.saitama-u.ac.jp)
Saitama University
Mizanur Rahman
Saitama University
Akihiko Matsuo
Saitama University
H. Damitha L. Abeynayaka
Saitama University

Article

Keywords: cyanobacteria, hydrogen peroxide, photoinhibition, diurnal behaviors, antioxidant activity, oxidative stress

Posted Date: April 11th, 2022

DOI: https://doi.org/10.21203/rs.3.rs-1529688/v1

Abstract

Diurnal variations of the oxidative stress condition of cyanobacteria were measured by field observations and laboratory experiments. In the field experiment, on clear summer days, transparent bottles, filled with surface water, were set up near the water surface, and several depths to 1 m deep. One bottle from each depth was collected every three hours together with the measurement of the photosynthetically active radiation (PAR). In the laboratory experiment, two cyanobacterial species were exposed to gradually increasing then decreasing light intensities. The samples were analyzed with the hydrogen peroxide (H_2O_2) concentration, the catalase activities (CAT), protein and chlorophyll a (Chl-a) contents. Regardless of difference in cyanobacterial species, similar diurnal trends were obtained. Protein contents did not change for one day experiments. Biologically generated H_2O_2 increased following the PAR intensity variation, with the delay of a few hours. The H_2O_2 concentration per protein was given as an increasing function of the exposure period (T) to the PAR. The amount of Chl-a content declined with the H_2O_2 per protein value.

The model was developed to estimate the H_2O_2 per protein value, elucidating that the effect of the cyanobacterial biomass and the surface layer mixing on the oxidative stress and mortality.

Introduction

Cyanobacteria are photosynthetic prokaryotes found in all habitats, and these organisms play a significant role in maintaining the ecological balance of nature. Like other organisms, cyanobacteria face an array of abiotic and biotic stresses from the environment, including metal ion toxicity, salinization, temperature, light conditions, eutrophication, allelopathy, and pathogens[1]. As an adaptive mechanism, cyanobacteria, and other species, exhibit various responses in morphology, biochemistry, physiology, and anatomy to counter these stresses. Among these responses, biochemical responses have widely been used as biomarkers to detect the stress on organisms[2,3]. The concentration of reactive oxygen species (ROS), activity of antioxidant enzymes, amino acid profile, and gene expression are some of the biomarkers employed in stress detections in aquatic plants, algae, and cyanobacteria.

As with other organisms, ROS accumulation causes harmful impacts on cyanobacteria, such as protein denature, impaired photosynthesis, growth inhibition, and anatomical damage[4,5], although ROS are important for growth regulation and signaling mechanisms[6,7]. When biological systems produce ROS in their metabolism[6], biological systems can control excess ROS production with the inherent scavenging enzymes and nonenzymatic components[2, 6, 8–10]. ROS production exceeds its scavenging capacity under a stress environment, consequently, ROS accumulate inside cells, and induces oxidative stress.

One of the most prominent ROS is H_2O_2. The observed H_2O_2 concentration of a water body is widely distributed, and the production rate is enhanced by the nutrient content of the water body[11]. Hence, the light intensity also is an important factor for the growth of cyanobacteria[12, 13].

Cyanobacteria are sensitive to even a minor change in light intensity causing stress for them[14]. Cyanobacteria can conduct photosynthesis and respiration via an elaborate electron transport pathway[15]. Collecting solar energy at photosystem II (PSII) in the thylakoid membrane results in the oxidation of water molecules and the reduction of plastoquinone, a molecule involved in the electron transport chain. The produced electrons are transported to PSI, where they are consumed in the synthesis of carbohydrates. An overabundance of solar energy results in the generation of ROS, including superoxide radicals, as the energy transfer rate is limited due to the underutilization of energy absorbed by the PSII antennae complex in the PSII reaction center[16, 17], and damages cellular components, such as D1 protein, which otherwise recovers the damaged photosynthesis apparatus[2, 18, 19]. Superoxide dismutase (SOD) catalyzes superoxide radicals into H_2O_2, which is then detoxified into water by antioxidant activities[20]. This mechanism has been intensively studied in the last two decades for many species, including cyanobacteria[4, 6, 9].

The H_2O_2 content and the activity of H_2O_2 scavenging enzymes can be used as good measures to detect the stress levels of these organisms. The physiological condition of cyanobacteria is highly dependent on the H_2O_2, content per protein ratio (Asaeda et al) [21].

Cyanobacteria is more vulnerable to H_2O_2 toxicity than another phytoplankton[22–24]. Advancement in artificial endorsement of H_2O_2 has been considered to suppress cyanobacteria bloom in natural water[22,25,26,27].

Associated with increasing solar radiation, H_2O_2 is intensively generated biologically[28–30], and high irradiance at the surface layer makes a significant impact on cyanobacterial physiology via H_2O_2 production.

At the same time, in natural water, H_2O_2 is produced by the photolysis of dissolved organic carbon (DOC) by UV[31–34]. Therefore, naturally generated H_2O_2 may have a possibility to contribute the decline of cyanobacteria.

The intensity of solar radiation changes diurnally, and cyanobacteria, under these changing light conditions, may have differing capacities to scavenge the ROS[34, 36], consequently, may exhibit the different damages in the diurnal variations.

Although the focus of the literature has been on the role of ROS, especially H_2O_2 in plants, in responding to environmental stresses[37–39], the behavior of cyanobacteria under diurnal light regimes is not well documented. Thus, this research was designed to study (1) the effect of light regime changes on cyanobacteria, (2) the relationship between solar radiation, H_2O_2 concentrations, and the antioxidant enzyme activities of cyanobacteria, and (3) the possibility of applying an H_2O_2 concentration as a proxy to detect stress intensity in algal management.

Results And Discussion

Diurnal variation of protein contents is shown in Fig.1, compared with PAR intensity. The protein content was nearly twice as higher in 2019 than in 2020.

In both field and laboratory experiments, the total protein (TP) content was nearly constant throughout the experimental period regardless of protein content in the early morning (Fig. 1). A similar trend was obtained for the optical densities, OD_{730}. These results indicate that the cell density changed only slightly with time.

The trend ofH_2O_2 concentration presented in Fig.2 was similar between the laboratory and field experiments. Although the magnitude was different, light-induced H_2O_2 production clearly indicated that the H_2O_2production increased in parallel to the PAR increment in the morning, however, peaked at 14:00 to 15:00, which was after the peak in the highest solar radiation at 11:40.

In the laboratory experiment, theH_2O_2 concentration was highest at 15:00, later than the peak PAR intensity. Species specifically, it was slightly higher with *P.ambiguum* compared with *M.aeruginosa*. The maximum PAR intensity, whether 300 or 600mmol m^{-2} s^{-1}, did not affect thefluctuating trends of H_2O_2 concentration.

Fig. 3 postulates the H_2O_2 concentration increment from the early morning value, normalized by the TP content with respect to the PAR intensity.

In parallel to the increasing PAR in the morning, theH_2O_2 per protein increased with the decline of the increasing rate. In the afternoon, although PAR declined, theH_2O_2 per protein further increased for a while, achieving the peak value of 4, at around 15:00, then declined. Thus, it showed a large anti-clockwise hysteresis curve. The H_2O_2 concentration depends on the light intensity, and generally low in the lower level of the water body with the low light intensity.

The diurnal trend of CAT activity is shown as a function of H_2O_2concentration in Fig. 5.

The CAT activity gradually increased in the morning until 15:00, with a sharp peak, followed by a declining trend of the variation of H_2O_2concentration thereafter. The H_2O_2 and CAT activity of both species were positively correlated (*M. aeruginosa*, R= 0.865, and *P. ambiguous*, R= 0.910) and were statistically significant (p< .001). There was a similar trend with the field observation

(Fig. 4).

Although similar trends were observed for the activities of other antioxidant enzymes such as guaiacol peroxidase (POD), and ascorbate peroxidase (APX). However, CAT was by far the largest (CAT/POD~100-700, CAT/APX~30-300, data are not shown).

Species specifically, even though the APX activity hardly changed between *P. ambiguum* and *M. aeruginosa*, the CAT activity was comparatively several times higher in *M. aeruginosa* than in *P. ambiguum*.

Chl-a and protein contents slightly decreased in a day with increasingH_2O_2 per protein (R= -0.536, t= 3.03, $p < 0.01$ for Chl-a and R = -0.400, t = 2.09, $p < 0.05$) (Fig. 5).

H_2O_2 source under high solar radiation in the field

The same trend of H_2O_2 concentration of both the field and laboratory conditions indicates that the oxidative stress of cyanobacteria varies diurnally.

The H_2O_2 concentration rose up to the magnitude of 100–200nmol L^{-1} in both laboratory and field before exposure to PAR. In the field samples, it was about 100 nmol L^{-1} in 2019 and less than 10 nmol L^{-1} in 2020 before exposure to solar radiation in the morning. In the laboratory, it was approximately 80 mol L^{-1}. The life span of H_2O_2 is 4 to 20 h implies that some level of H_2O_2 concentration is maintained though daily production[40]. The H_2O_2 per protein in the early morning samples is likely attributed to the H_2O_2produced in the previous days, either biologically or by the photolysis of DOC.

Except for the H_2O_2 concentration in the early morning, the H_2O_2 concentration increased by 80 to 160 nmol L^{-1} at the highest radiation period (Fig. 2). This is the amount generated biologically exposed to the high solar radiation.

Although biomass was not measured in this study, one third to one half of the cyanobacteria biomass is composed of protein[41]. Thus, the H_2O_2 per protein value indicates two to three times the amount biologically generated by a single cell exposed to the PAR.

The maximum H_2O_2 amount corresponds to about 3 to 4 nmol H_2O_2 per protein (mg), indicating that about 1 nmol of H_2O_2 per biomass (mg) was generated and contained in the cells. Considering the nearly neutral buoyancy of the cyanobacteria biomass, the H_2O_2 concentration is equivalent to approximately 1mmol H_2O_2 L^{-1}.

Many studies have been conducted on the lethal H_2O_2 concentration of cyanobacteria, mainly via incubations in laboratories, with the endorsement of different concentrations of H_2O_2.

Specifically, the growth of cyanobacteria was suppressed with H_2O_2 concentrations of 30mmol L^{-1} [25,26], 100mmol L^{-1} [27], 118mmol L^{-1} [12], 325mmol L^{-1} [42], and 275mmol L^{-1} [43].

The maximum H_2O_2 concentration in the present study, 1nmol H_2O_2biomass^{-1} (mg) (~1mmol H_2O_2 L^{-1}), is several times higher than the lethal concentration of cyanobacteria.

H_2O_2 concentration was measured in other types of plant species, where approximately 1mmol H_2O_2 g^{-1}FW was reported, and the growth was inhibited over 10mmol $H_2O_2g^{-1}$FW[39, 44, 45].

Considering that cyanobacteria are more vulnerable to H_2O_2 toxicity than other plants, the lethal H_2O_2 concentration in the present study agrees well with other plants results.

In a day, the high H_2O_2 concentration period continued for several hours only and did not last long. Cyanobacteria in surface water is in the lethal condition during the period and Chl-a as well as protein contents substantially declined associated with the increasing H_2O_2 per protein (Fig. 4). In the present field observation, many dead cells were observed after the period.

Diurnal patterns of generation and detoxification of H_2O_2

Associated with the solar radiation intensity, the H_2O_2 per protein was fluctuatedin a day. H_2O_2 is catalyzed majorly by the CAT activity, the activity of which is associated with the amount of H_2O_2 after transmitted by the signal[46-48]. The high correlation between the H_2O_2 concentration and antioxidant activities indicates that the signal transmission of elevated H_2O_2 concentration is relatively quick[7].

Although the light intensity sharply changed from the increasing phase to a decreasing phase at 11:40, the H_2O_2 concentration continued to rise slightly later, until around 15:00, and then gradually turned into the decreasing phase (Fig. 2).

Similar to this study, a one-hour delay from the solar radiation peak was observed in the photosynthetic quantum yield of the *Microcystis* bloom in Lake Taihu[49,50]. As the mechanism is unknown, the effect is empirically estimated.

The H_2O_2 production rate was relatively low with the same intensity PAR in the afternoon. With morning and afternoon values together, the produced H_2O_2 per protein is assimilated as a function of PAR, such as

$$H_2O_2\ \text{protein}^{-1} = PAR^{0.21} \quad (1)$$

($R = 0.732$, $t = 4.05$, $p < 10^{-3}$).

Fig. 6 shows the observed H_2O_2 protein^{-1} normalized by equation (1), E (= $PAR^{0.21}$), as a function of the period from 6:00, T (hrs.). There was a significant increasing trend for the normalized H_2O_2 protein^{-1}, and is assimilated by

$$E = 1.2*\sin(p*(T-3)/24)^2 \quad (2)$$

($R = 0.743$, $t = 6.38$, $p < 10^{-6}$)

The evaluation of H_2O_2 per protein

The solar radiation is reflected at the water surface and attenuated in water.

The PAR intensity above the water surface is approximately given by

$I_0(T) = I_0 \cos(q)$ (3)

whereqis the incident angle of the solar radiation, approximately given by abs ((12 – T)p/12), and T is hrs. from 6:00.

Reflection coefficient at the water surface, Fr, is approximately given by

$Fr = F_0 + (1- F_0)\ (1-\cos(q))^5$(4)

Thus, the PAR intensity at time, T, and the depth, z, is provided by

$I(T, z) = I_0(T)\ (1-Fr) \exp(-kz)$(5)

Where $I_0(T)$ is the PAR intensity just below the water surface, z is the depth (m), k is the extinction coefficient of water (1 m^{-1}), given as a function of cyanobacteria biomass (protein content), or the protein content, given as

k = 0.25* Protein (1 m^{-1}) (6)

where Protein is the protein content in mg L^{-1} (R= 0.807, t= 3.87, $p < 0.01$).

The PAR in water was obtained with sufficient agreement (R = 0.900, t = 6.72, $p < 10^{-4}$ for 2019; R = 0.620, t = 2.98, $p < 0.01$ for 2020).

Simulated H_2O_2 $protein^{-1}$ by equation (2) is postulated in Fig. 7, compared with the observed values.

The sufficient agreement was achieved (R = 0.705, t =3.30, $p < 0.001$ for 2019; R = 0.728, t = 5.10, $p < 10^{-5}$ for 2020).

In stagnant water, thermal stratification forms near the surface by the supplied solar energy from the surface. However, due to the disturbances, such as wind or cooling, the close to the surface is often mixed, where cyanobacteria distribution becomes relatively homogeneous.

H_2O_2 per protein in the mixed layer is postulated as a function of protein contents, 5, 10, and 30 mg L^{-1}, and thickness of the mixed layer, 0.1, 0.2 and 0.5m, in Fig. 8. At the surface, H_2O_2 per protein is independent of protein contents.

The H_2O_2 per protein value decreases with increasing mixed layer thickness, as the light intensity is attenuated in the deep layer. With low density of cyanobacteria, or low protein density, such as 5 to 10 mg L^{-1}, the H_2O_2 per protein values do not decrease much even deeply mixed because the light intensity is

high in the deep layer due to the low attenuation rate. While with high density of cyanobacteria, H_2O_2 per protein substantially declines with increasing thickness of the mixed layer. This indicates that the mortality rate of cyanobacteria is higher with low density and is suppressed by rising cyanobacterial biomass.

The vertical migration of cyanobacteria

Lake cyanobacteria exhibit vertical migration behavior as an ecological strategy to minimize predation pressure, nutrient limitations, competition, and so forth[51-55]. In most cases, cyanobacteria move to the deepest layers of the water body from 12:00 to 18:00, slightly later than the highest solar radiation period, and gradually rise thereafter. The present results indicate that the highest H_2O_2 protein^{-1} occurs slightly later than the highest light time. The H_2O_2 concentration gradually lowers due to antioxidant activities afterwards. The cyanobacteria stay in the deeper zone in the early afternoon, likely to avoid the high solar radiation and the oxidative stress before the recovery of homeostasis by the increasing antioxidant activities[52].

The effect of the species specific detoxification rate

In response to light intensity, *M. aeruginosa* has lower SOD activity per protein under the same light intensity compared with *P. ambiguum*. The generation rate of superoxide seems to be low in *M. aeruginosa*, likely because of the aggregation and forming scums of *M. aeruginosa* cells and being embedded by mucilage. These systems probably limit the light intensity, substantially weakening it by the time it arrives at the cell[48, 55].

The CAT activity per protein was twice to thrice times higher in *M. aeruginosa* than that of *P. ambiguum*for the same H_2O_2 concentration. Although CAT is not a unique enzyme to catabolize H_2O_2, H_2O_2 was broken down more intensively into water and oxygen by *M. aeruginosa* than *P. ambigum*. Thus, the H_2O_2 concentration was lower with *M.aeruginosa* than with *P.ambiguum* in the period of high solar radiation. *M. aeruginosa* is reported to be weak under high H_2O_2concentration[56]. However, together with higher antioxidant activities, it might exhibit a higher level of tolerance against light intensity than *P. ambiguum*, and it seems to enable *M.aeruginosa* to be dominant in the surface water under high solar radiation.

The efficiency of the destratification system on the blooming of these species

In the destratification system, to reduce algal biomass, the passive migration of algae into the deep layer by mechanical enforcement, such as artificial mixing, wind mixing, and night-time convection, is expected to prevent photosynthesis[57-59]. The present study indicates a strong photoinhibition of cyanobacteria under solar radiation near the surface.As a result, slightly low light conditions are best for enabling cyanobacteria to grow. Compared with *P.ambiguum*, the destratification system will work more efficiently with *M. aeruginosa*, as it has a high tolerance to high solar radiation. However, the algal biomass can

only be sufficiently reduced at a certain depth of the destratification layer. It is suggested that further studies estimate such aspects to potentially help to manage cyanobacterial blooms.

Conclusions

Regardless of difference in cyanobacterial species, similar diurnal trends were obtained. Protein contents did not change for one day experiments. Biologically generated H_2O_2 increased following the PAR intensity, with an approximately two to three-hour delay of the PAR exposure. Therefore, the oxidative stress indicator, the H_2O_2 concentration per protein showed the large hysteresis with respect to daytime PAR intensity variation, lower in the morning than in the afternoon with the same PAR intensity and is given as an increasing function of the T to the solar radiation. The amount of Chl-a concentration declined with increasing H_2O_2 per protein value. CAT activity, far largest compared with other antioxidant activities, solely follows the H_2O_2 concentration. Using these relationships, the prediction model to estimate H_2O_2 per protein value was developed with sufficient agreement with observation.

It was elucidated that the biologically generated H_2O_2 concentration was in the lethal level of cyanobacteria in the surface layer during high solar radiation period, and high biomass of cyanobacteria declines PAR intensity in water and avoids the oxidative stress.

These results indicate that H_2O_2 would be an effective biomarker to detect the stress level of cyanobacteria; the addition of H_2O_2 to freshwater may prove beneficial in designing the criteria for cyanobacteria management.

Methodology

Ethical permission

This study has been approved by the Ministry of Environment of Japan (H30 Kokyo-Gaienbori ni okeru Kyokushoteki Ihicjiteki Aoko Taisaku-Gijutu Jisshou-Gyomu (Chidorighuchi Hibiyabori) ni Kakawaru Kikaku-Teian).

Field observation

Diurnal sampling in the field was performed. Field observations were made on a clear windless day on August 17, 2019, and August 29, 2020, at the boat jetty of the Chidorigafuchi moat of the Imperial Palace, Japan (35^o 41’40” N; 139^o 45’20” E) (Fig. 9). The moat was 2.5m deep in average. The highest solar radiation was observed at 11:40. Before 6:00, six semi cubic transparent bottles filled with surface water were set up at different depths, surface water (in 2020 experiment only), 0.1m, 0.3m (in 2020 experiment only), 0.5 m, and 1.0 m (in 2019 experiment only). At 9:00, 12:00, 15:00, 18:00 and 21:00, one bottle was collected from each depth and stored in a cool box (~0 ^{o}C) for transporting to the laboratory. At 13:30,

another bottle was also collected, but only from a depth of 0.1m to see the effect of high solar radiation. Because all of the water is subject to convection during the night, the water was homogeneous at 6:00.

At each sampling time, light intensity, i.e., photosynthetically active radiation (PAR), was measured at each depth, along with temperature, pH, conductivity, and dissolved oxygen content (DO), by using a light intensity meter (Apogee, MQ-200, United States) and water quality meter (U-51, Horiba, Kyoto, Japan). On the observation day, the temperature was in the range of 28.3 ^{o}C to 32.6 ^{o}C in 2019, and 30.5 ^{o}C to 32.9^{o}C in 2020, while the pH fluctuated from 8.22 to 8.49 in 2019 and 8.85 to 9.45 in 2020. The turbidity changed from 91.8 to 99.6 NTU in 2019 and 27.5 to 30.2 NTU in 2020, and the conductivity varied from 21.1 to 25.5 ms/m in 2019 and 28.6 to 30.2 ms/m in 2020. The water samples were rich in *Anabaena flos-aquae*: the density at the surface and at 50 cm was 11,800 cells mL^{-1} (81% of all the cells) and 4500 cells mL^{-1} (49% of all the cells), respectively, in 2019. *Microcystis aeruginosa* had a density of 55,300 cells mL^{-1} (95% of all the cells) at the surface and 34,500 cells mL^{-1} (90% of all the cells) at 50 cm, respectively, in 2020.

Laboratory Experiments

The laboratory experiments were conducted with more accurate condition, to confirm the rend observed in the field experiment.

Phormidium ambiguum (N2119) and *Microcystis aeruginosa* (N111) were obtained from the National Institute of Environmental Studies (NIES), Japan. These two strains were cultured and acclimatized for 14 days in an autoclaved BG 11 medium[60].

All experiments were conducted by using incubators (MIR-254, Sanyo, Tokyo, Japan) and in the nutrient level of BG-11 for 14 days at 20 ^{o}C with a 12h:12h light-and-dark (25 µmol s^{-1}m^{-2}) cycle, using a VBP-L24-C2 light source (Valore, Kyoto, Japan).

Each culture was divided into 36 flasks (10 ml) which were used as experimental units. During the experiment, the cultures were exposed to two levels of light: the intensity shifted from 0 µmol m^{-2} s^{-1} at 6:00 to either 300 µmol m^{-2} s^{-1} at 12:00 or 600 µmol m^{-2} s^{-1} at 12:00 by changing the intensity to intervals of 25mmol m^{-2} s^{-1} or 50 µmol m^{-2} s^{-1}, respectively. Then, the light intensity was decreased at the same rates until 18:00. The temperature was kept constant (20 ^{o}C) throughout the experiment. Every three hours, (i.e., at 6:00, 9:00, 12:00, 15:00, 18:00, and 21:00), three flasks were taken for a stress response analysis, while the remaining experimental units were manually shaken. The collected samples were subjected to bioassays, which are described later. The experimental units per each light condition were triplicated to confirm reproducibility.

Analyses

Chlorophyll concentration analysis

To begin, 10 mL of a homogenized treated cell suspension was centrifuged for 10 min at 3000 rpm, and the supernatant was removed. The cell pellet was washed using Milli-Q water, and then it was dried in a vacuum chamber. The dried pellet was vortexed using 3 mL of absolute acetone to dissolve it. Pigments of chlorophyll-a (Chl-a) were spectrophotometrically (UVmini-1240, Shimadzu, Japan) measured after being extracted into N,N-dimethylformamide by keeping them in darkness for 24 h[61], and the specific extinction coefficient of 92.6 mL $mg^{-1}cm^{-1}$ at 663 nm for Chl-a was employed[62].

Identification of cells and the cell density measurement

A small aliquot of 1 mL of each treated cell suspension was fixed at room temperature for 2 h using glutaraldehyde solution, and it was stored at 4 °C for counting. Cell identification and their densities were obtained by counting the fixed cyanobacterial cells using a light microscope supported with a digital camera (Nikon DXM 1200C) at its highest resolution (4116 x 3072 pixels), equipped with a bacteria-counting chamber with a depth of 0.02 mm (SLGC, Japan).

To estimate the growth of cyanobacteria, the OD_{730} was measured by taking 1 mL of sample from each flask. The OD_{730} was measured with a UV–Vis spectrophotometer (UVmini-1240, Shimadzu, Kyoto, Japan) at an optical absorption wavelength of 730 nm, using a previously proposed methodology[63].

Total protein content analysis

In the same manner as the chlorophyll measurements, the cyanobacterial cells were harvested. Then TP was measured using the same method that was mentioned in[64], with minor modifications. After treating the cyanobacterial growth media, the cells were separated by centrifugation at 4 °C for 20 min at 10,000 rpm. After the pellet was washed once with distilled water, it was subjected to a freeze-thaw cycle and then grounded, using a motor. The total protein was extracted using a 0.5 M NaOH solution, and the extraction was centrifuged at 4 °C for 20 min at 10,000 rpm. The supernatant was used as crude protein extract, and the protein content was quantitatively analyzed with the aid of a Coomassie Bradford protein assay kit. The crude protein extract was stained with Coomassie (G-250) dye and incubated for 10 min at room temperature, and then the absorbance was measured at 595 nm using a spectrometer. The protein content was determined using a known concentration series of Albumin.

Stress assay

Enzyme extraction

The stress assays were performed by detecting the concentration of H_2O_2 and the activities of the antioxidant enzymes of catalase (CAT), superoxide dismutase (SOD), ascorbic peroxidase (APX), and peroxidase (POD). For the stress assays, the cells were extracted into an ice-cold phosphate buffer (pH 6.0, 50 mM) that contains polyvinylpyrrolidone (PVP) and masks the effect of phenolic compounds. Then, the extractions were centrifuged at 5,000 × *g* at 4 °C for 15 min. The supernatant was separated

and incubated at -80 °C until further analysis. For each treatment, the extractions were performed in triplicate. All the results are expressed in protein basis.

H_2O_2 Assay

The cellular H_2O_2 contents were estimated according to the e-FOX method[65], and the $TiClO_4$ method[66].

In e-FOX method, 1ml of the sample was taken from the flask and the supernatants were removed by centrifugation at 10,000 × g for 10 min at 4 °C. To extract the cellular H_2O_2, the cell pellets were homogenized in 1 mL of 0.1 M pH 7.0 phosphate buffer and centrifuged at 10,000 × g for 10 min at 4 °C. 25mM of ferrous ammonium sulfate is mixed with 20% H_2SO_4 to make reagent A alongside reagent B (sigma aldrich Co. Ltd) is prepared with help of 0.1M D-sorbitol, 0.125mM xylenol orange using Milli-Q water to make its final volume. A mixture of 1ml reagent B and an equal volume of 10µL reagent A and ethanol (99.5%) is used for a single analysis. The optical absorption mainly the xylenol orange complex that forms with oxidized metals such as ferric iron was measured at 560 nm using a spectrophotometer (UVmini-1240).

In $TiClO_4$ method, 1 mL was collected from each flask, and the supernatants were removed by centrifugation at 10,000 × *g* for 10 min at 4 °C. The cell pellets were washed once with ultrapure water (Milli-Q direct 5, Merck KGaA, Darmstadt, Germany). To extract the cellular H_2O_2, the cell pellets were homogenized in 1 mL of 0.1 M pH6.5 phosphate buffer and centrifuged at 10,000 × *g* for 10 min at 4 °C. A total of 750 µ L of 1% Titanium chloride in 20% H_2SO_4 (v/v) was then added to initiate the reaction. The optical absorption was measured at 410 nm using a spectrophotometer (UVmini-1240), following centrifugation (10,000 × *g* for 5 min) at room temperature (25 ± 2 °C).

The H_2O_2 concentration was determined using a standard curve of the optical absorption, prepared using a series of samples with known H_2O_2 concentration. However, the absorption at 560nm or 410 nm may have a possibility to include the effect of other soluble compounds[65, 67, 68]. Thus, the H_2O_2 concentration was calculated from the slope of the standard curve obtained from the known H_2O_2 concentration, which was offset, derived by the intercept absorption rate with zero H_2O_2 concentration samples[67].

The results were compared with the results of both analyses, and suitable agreement was obtained (R = 0.85)[65].

CAT, APX, and POD activity assays

In the CAT activity assay, a total of 1 mL of each culture was centrifuged at 10,000 × *g* at 4 °C for 10 min. The supernatant was removed, and the cell pellets were homogenized in 1 mL potassium phosphate buffer (50 mM, pH 7.0), containing 0.1 mM EDTA. After centrifuging again (10,000 × *g* at 4 °C for 10 min), the supernatant was collected as the enzyme extract. The CAT activity was measured by reacting 15 µL of 750 mM H_2O_2, 920 µL of potassium phosphate buffer, and 65 µL of extract supernatant. Optical

absorption was measured at 240 nm using UV mini-1240. The measurements were recorded every 10 s for 3 min, and the CAT activity was calculated using an extinction coefficient of 39.4 $mM^{-1}cm$[69].

For the APX assay, the reaction mixture contained 100 µL of enzyme extract, 200 µL of 0.5 mM ascorbic acid in 50 mM of potassium phosphate buffer (pH 7.0), and 2 mL of 50 mM potassium phosphate buffer (pH 7.0), mixed with 60 µL of 1 mM H_2O_2. The decrease in absorbance at 290 nm was recorded every 10 s for 3 min. The APX activity was calculated using an extinction coefficient of 2.8 mM^{-1} cm^{-1},[70].

The POD activity was assayed following[71], with slight modifications. The cyanobacteria cells were harvested by centrifuging 1-mL samples at 10,000 × *g* at 4 °C for 10 min and removing the supernatant and cell pellets, which were homogenized in 1 mL of potassium phosphate buffer (100 mM, pH 7.0). A total of 65 µl of enzyme extract was then mixed with 920 µL of potassium phosphate buffer (100 mM, pH 7) containing 20 mM of guaiacol. With the addition of 15 µL of 0.6% H_2O_2, the absorbance change was then recorded at 470 nm every 10 s for 3 min using UV mini-1240. POD activity was calculated with an extinction coefficient of 26.6 mM/cm.

Statistical analyses

The collected data were tested for normality with the Shapiro–Wilk's test before the statistical analyses. All results were presented as the mean ± SD (n = 3). The data were subjected to a two-way analysis of variance (ANOVA), and the bivariate analysis was used and followed by Pearson's correlation method to evaluate the relationship among the parameters. The statistical analyses were performed with IBM SPSS V25.

Declarations

Author contributions

T.A. contributed to the design of the experiment, observation, and writing the manuscript.

M.R. contributed to the revision of the manuscript.

A.M. carried out filed sampling and analyses.

D.H.L.A. carried out the experiment and analyses.

Acknowledgement

This work was financially supported by the Grant-in-Aid for Scientific Research (B) (19H02245) and Fund for the Promotion of Joint International Research (18KK0116) of Japan Society for the Promotion of Science (JSPS).

Conflicts of Interest

The authors declare no conflict of interest.

Data availability statement

The authors highly appreciate and stated that data is available for everyone in supplementary file named ‘Raw data.’

References

1. Ma, J., Wang, P. Effects of rising atmospheric CO_2 lavels on physiological response of cyanobacteria and cyanobacteria bloom development: A review. Sci. Total. Env. **754**, 141889 (2021).
2. Gill, S.S., Tuteja, N. Reactive oxygen species and antioxidant machinery in abiotic stress tolerance in crop plants. Plant Physiol. Biochem. **48**, 909–930 (2010).
3. Atapaththu, K.S.S., Asaeda, T. Responses of aquatic macrophytes to flucuations in abiotic stress vectors. In: Crystal, E., Rodney (Ed.), Aquatic Plants Composition, Nutrient Concentration and Environmental Impact. Nova, New York (2015).
4. Ma, Z., Gao, K. Spiral breakage and photoinhibition of Arthrospira platensis (Cyanophyta) caused by accumulation of reactive oxygen species under solar radiation. Environ. Exp. Bot. **68**, 208–213 (2010).
5. Diaz, J.M., Plummer, S. Production of extracellular reactive oxygen species by phytoplankton: past and future directions. J. Plank. Res. **40**, 655–666 (2018).
6. Rastogi, R.P., Singh, S.P., Häder, D.-P., Sinha, R.P. Detection of reactive oxygen species (ROS) by the oxidant-sensing probe 2',7'-dichlorodihydrofluorescein diacetate in the cyanobacterium Anabaena variabilis PCC 7937. Biochem. Biophys. Res. Commun. **397**, 603–607 (2010).
7. Foyer, C.H. Reactive oxygen species, oxidative signaling and the regulation of photosynthesis. Environ. Exp. Bot. **154**, 134–142 (2018).
8. Caverzan, A., Passaia, G., Rosa, S.B., Ribeiro, C.W., Lazzarotto, F., Margis-Pinheiro, M. Plant responses to stresses: Role of ascorbate peroxidase in the antioxidant protection. Genet. Mol. Biol. **35**, 1011–1019 (2012).
9. Sharma, P., Jha, A.B., Dubey, R.S., Pessarakli, M. Reactive oxygen species, oxidative damage, and antioxidative defense mechanism in plants under stressful conditions. J. Bot. (2012).
10. Ugya, A.Y., Imam, T.S., Li, A., Ma, J., Hua, X. Antioxidant response mechanism of freshwater microalgae species to reactive oxygen species production: A mini review. Chem. Ecol. **36**, 174–193 (2020).
11. Herrmann, R. The daily changing pattern of hydrogen peroxide in New Zealand surface waters. Environ. Toxicol. Chem. **15**, 652–662 (1996).
12. Mikula, P., Zezulka, S., Jancula, D., Marsalek, B.. Metabolic activity and membrane integrity changes in *Microcystis aeruginosa*–New findings on hydrogen peroxide toxicity in cyanobacteria. Eur. J. Phycol. **47**, 195–206 (2012).

13. Dalu, T., Wasserman, R.J. Cyanobacteria dynamics in a small tropical reservoir: Understanding spatio-temporal variability and influence of environental variables. Sci. Total Env. **643**, 835–841 (2018).
14. Beecraft, L., Watson, S.D., Smith, R.E.H. Innate restance of PSII efficienty to sunlight stress is not ans advantage for cyanobacteria comapred to eukaryotic phytoplankton. Aquat. Ecol. **53**, 347–364 (2019).
15. Lea-Smith, D.J., Bombelli, P., Vasudevan, R., Howe, C.J. Photosynthetic, respiratory and extracellular electron transport pathways in cyanobacteria. Biochim Biophys Acta. **1857**, 247–255 (2016).
16. Latifi, A., Ruiz, M., Zhang, C.-C.. Oxidative stress in cyanobacteria. FEMS Microbiol. Rev. **33**, 258–278 (2009).
17. Raja, V., Majeed, U., Kang, H., Andrabi, K.I., John, R. Abiotic stress: Interplay between ROS, hormones and MAPKs. Environ. Exp. Bot. **137**, 142–157 (2017).
18. Nishiyama, Y., Murata, N. Revised cheme for the mechanism of phtoinhibition and its application to enhance the abiotic stress tolearance of the photosyntetic machinery. Appl. Microbiol. Biotechnol. **98**, 8777–8796 (2014).
19. Weerakoon, H.P.A.T., Atapathu, K.S.S., Asanthi, H.B. Toxicity evaluation and environmental risk assessment of 2-methyl-4-chlorophenoxy acetic acid (MCPA) on non-target aquatic macrophyte Hydrilla verticillata. Environ. Sci. Pollut. Res. **25**, 30463–30474 (2018).
20. Asada, S., Fukuda, K., Oh, M., Hamanishi, C., Tanaka, S. Effect of hydrogen peroxide on the metabolism of articular chondrocytes. Inflamm. Res. **48**, 399–403 (1999).
21. Asaeda, T., Rahman, M., Abeynayaka, H.D.L., 2022. Hydrogen peoxide can be a plausible biomarker in cyanobacterial bloom treatment. Scietific Report **12**:12 (2022).
22. Drábková, M., Matthijs, H., Admiraal, W., Maršálek, B. Selective effects of H_2O_2 on cyanobacterial photosynthesis. Photosynthetica **45**, 363–369 (2007).
23. Drábková, M., Admiraal, W., Maršálek, B. Combined exposure to hydrogen peroxide and light selective effects on cyanobacteria, green algae, and diatoms. Environ. Sci. Technol. **41**, 309–314 (2007).
24. Jančula, D., Drábková, M., Černý, J., Karásková, M., Kořínková, R., Rakušan, J., Maršálek, B. Algicidal activity of phthalocyanines— Screening of 31 compounds. Environ Toxicol. **23**, 218–22 (2008).
25. Barrington, D.J., Ghadouani, A. Application of hydrogen peroxide for the removal of toxic cyanobcteria and other phytoplankton from waste water. Environ. Sci. Technol. **42**, 8916–8921 (2008).
26. Barrington, D.J., Reichwaldt, E.S., Ghadouani, A. The use of hydrogen peroxide to remove cyanobacteria and microcystins from waste stabilization ponds and hypereutrophic systems. Ecol. Engg. **50**, 86–94 (2013).
27. Leunert, F., Eckert, W., Paul, A., Gerhardt, V., Grossart, H. P. Phytoplankton response to UV-generated hydrogen peroxide from natural organic matter. Journal of Plankton Research. **36**, 185–197 (2014).

28. Dubinsky, Z., Berman, T. Light utilization by phytoplankton in Lake Kinnert (Islael). Limnology and Oceangraphy **26**, 660–670 (1981).
29. Foy, R. Interaction of temperature and light on the growth rates of two planktonic Oscillatoria species under a short photoperiod regime. British Phycological J. **18**, 267–273 (1983).
30. Tilzer, M.M. Light-dependence of photosynthesis and growth in cyanobacteria: Implications for their dominance in eutrophic lakes. N. Z. J. Mar. Freshw. Res. **21**, 401–412 (1987).
31. Cooper, W.J., Lean, D.R.S. Hydrogen peroxide concentration in a northern lake: Photochemical formation and diel variability. Environ Sci Technol. **23**, 1425–1428 (1989).
32. Scully, N., McQueen, D., Lean, D. Hydrogen peroxide formation: The interaction of ultraviolet radiation and dissolved organic carbon in lake waters along a 43–75 N gradient. Limnol. Oceanogr. **41**, 540–548 (1996).
33. Häkkinen, P.J., Anesio, A.M., Granéli, W. Hydrogen peroxide distribution, production, and decay in boreal lakes. Can J Fish Aquat Sci. **61**, 1520–1527 (2004).
34. Garcia, P.E., Queimalinos, C., Dieguez, M.C. Natural levels and photo-production rates of hydrogen perooxide (H_2O_2) in Andean Patagonian aquatic sysyems: Influence of the dissolved organic matter pool. Chemosphere **217**, 550–557 (2019).
35. Tanaka, K., Nakanishi, S. Time-of-day dependent responses of cyanobacterial cellular viability against oxidative stress. BioRxiv, 851774 (2019).
36. Welkie, D.G., Rubin, B.E., Diamond, S., Hood, R.D., Savage, D.F., Golden, S.S. A hard day's night: Cyanobacteria in diel cycles. Trends Microbiol. **27**, 231–242 (2019).
37. Asaeda, T., Barnuevo, A. Oxidative stress as an indicator of niche-width preference of mangrove Rhizophora stylosa. For. Ecol. Man. **432**, 73–82 (2019).
38. Asaeda, T., Senavirathna, M.D.H.J., Vamsi Krishna, L., Yoshida, N. Impact of regulated water levels on willows (*Salix subfragilis*) at a flood-control dam, and the use of hydrogen peroxide as an indicator of environmenal stress. Ecol. Engg. **127**, 96–102 (2019).
39. Asaeda, T., Senavirathna, M.D,H.J., Vamsi Krishna, L. Evaluation of habitat preference of invasive macrophyte *Egeria densa* in different channel slopes using hydrogen peroxide as an indicator. Front. Plant Sci. 11.422, doi:10.3389/fpls.2020.00422 (2020).
40. Cooper, W.J., Lean, D.R.S. Hydrogen peroxide dynamics in marine and freshwater systems. Encyclopedia of Earth System Science **2**, 527–535 (1992).
41. Lopez, C.V.G., García, M.D.C.C., Fernández, F.G.A., Bustos, C.S., Chisti, Y. & Sevilla, J.M.F. Protein measuremements of microalgae and cyanobacterial biomass. Bioresour Technol **101**(**19**), 7587–7591 (2010)
42. Ding, Y., Gan, N., Li, J., Sedmak, B., Song, L. Hydrogen peroxide induces apoptotic-like cell death in *Microcystis aeruginosa* (Chroococcales, Cyanobacteria) in a dose-dependent manner. Phycologia. **51**, 567–575 (2012).

43. Foo, S.C., Chapman, I.J., Hartnell, D.M., Turner, A.D. & Franklin D.J. Effects of H_2O_2 on growth, metabolic activity and membrane integrity in three strains of *Microcystis aeruginosa*. Env Sci Poll Res **27**(**31**), 38916–38927 (2020)
44. Asaeda, T., Rashid, M.H., & Schoelynck, J. Tissue hydrogen peroxide concentration can explain the invasiveness of aquatic macrophytes: A modeling perspective. Front Environ Sci **8**, 292 (2021)
45. Asaeda, T., Rahman, M., Liping, X., Schoelynck, J., 2022. Hydrogne peroxide variation patterns as abiotic stress responses of *Egeria densa*. Frontiers in Plant Sci. (2022).
46. Vesterkvist, P.S.M., Misiorek, J.O., Spoof, L.E.M., Toivola, D.M., Meriluoto, J.A.O. Comparative cellular toxicity of hydrophilic and hydrophobic microcystins on caco-2 cells. Toxins **4**, 1008 (2012).
47. Preece, E.P., Hardy, F.J., Moore, B.C., Bryan, M. A review of microcystin detections in estuarine and marine waters: Environmental implications and human health risk. Harmful Algae **61**, 31–45 (2017).
48. Pham, T.-L., Utsumi, M. An overview of the accumulation of microcystins in aquatic ecosystems. J. Environ. Manag. **213**, 520–529 (2018).
49. Wu, X., Kong, F., Zhang, M. Photoinhibition of colonial and unicellular *Microcystis* cells in as summe bloom in Lake Taihu. Limnology **12**, 55–61 (2011).
50. Chen, L., Chen, J., Zhang, X., Xie, P. A review of reproductive toxicity of microcystins. J. Hazard. Mater. **301**, 381–399 (2016).
51. Molle, F., Renwick, M. Economics and politics of water resources development: Uda Walawe Irrigation Project, Sri Lanka.. Research Report 87. IWMI, Colombo, Sri Lanka (2005).
52. Athukorala, D., Amarasinghe, U. Status of the fisheries in two reservoirs of the Walawe river basin, Sri Lanka: A case of participation of fishers in management. Asian Fish. Sci. **23**, 284–300 (2010).
53. Cañedo-Argüelles, M., Kefford, B.J., Piscart, C., Prat, N., Schäfer, R.B., Schulz, C.-J. Salinisation of rivers: An urgent ecological issue. Environ. Pollut. **173**, 157–167 (2013).
54. McLellan, N.L., Manderville, R.A. Toxic mechanisms of microcystins in mammals. Toxicol. Res. **6**, 391–405 (2017).
55. Drobac, D., Tokodi, N., Lujić, J., Marinović, Z., Subakov-Simić, G., Dulić, T., Važić, T., Nybom, S., Meriluoto, J., Codd, G.A., Svirčev, Z. Cyanobacteria and cyanotoxins in fishponds and their effects on fish tissue. Harmful Algae **55**, 66–76 (2016)
56. Wang, B., Song, Q., Long, J., Song, G., Mi, W., Bi, Y. Optimization method for Microcystis bloom mitigation by hydrogen peroxide and its stimulative effects on growth of chlorophytes. Chemosphere **228**, 503–512 (2019).
57. Visser, P.M., Ibelings, B.W., Bormans, M., Huisman, J. Artificial mixing to control cyanobacterial blooms: A review. Aquat. Ecol. **50**, 423–441 (2016).
58. Abeynayaka, H.D.L., Asaeda, T., Kaneko, Y. Buoyancy limitation of filamentous cyanobacteria under prolonged pressure due to the gas vesicle collapse. Env. Man. **60**, 293–303 (2017).
59. Abeynayaka, H.D.L., Asaeda, T., Rashid, M.H. Effects of elevated pressure on Pseudoanabaena galeata Bocher in varying light and dark environment. Env. Sci. Poll. Res. **25**, 21224–21232 (2018).

60. Rippka, R., Deruelles, J., Waterbury, J.B., Herdman, M., Stanier, R.Y. Generic assignments, strain histories and properties of pure cultures of cyanobacteria. Microbiol. **111**, 1–61 (1979).
61. Porra, R.J., Thompson, W.A., Kriedemann, P.E. Determination of accurate extinction coefficients and simultaneous equations for assaying chlorophylls a and b extracted with four different solvents: Verification of the concentration of chlorophyll standards by atomic absorption spectroscopy. Biochim. Biophys. Acta. Bioenerg. **975**, 384–394 (1989)
62. Ehling-Schulz, M., Bilger, W., Scherer, S. UV-B-induced synthesis of photoprotective pigments and extracellular polysaccharides in the terrestrial cyanobacterium Nostoc commune. J. Bacteriology **179**, 1940–1945 (1997).
63. Association, A.P.H.; Association, A.W.W.; Federation, W.P.C.; Federation, W.E. Standard Methods for the Examination of Water and Wastewater. American Public Health Association: Washington, D.C., USA; ISBN 8755-3546 (1915).
64. Dautania, G. K., and Singh. G.P.Role of Light and Dark Cycle and Different Temperatures in the Regulation of Growth and Protein Expression in *Oscillatoria agardhii* Strain. Brazilian Archives of Biology and Technology. 57, 933–940 (2014)
65. Queval, G., Hager, J., Gakiere, B., Noctor G. Why are literature data for H2O2 contents so variable? A discussion of potential difficulties in the quantitative assay for leaf extracts. J. Exp. Bot. **59**, 135–146 (2008).
66. Jana, S. & Choudhuri, M.A. Glycolate metabolism of three submersed aquatic angiosperms during ageing. Aquatic Botany 12, 345–354 (1982)
67. Veljovic-Jovanovic S., Noctor G. & Foer C.H. Are leaf hydrogen peroxide concentrations commonly overestimated? The potential influence of artefactual interference by tissue phenolics and ascorbate. Plant Physiol Biochem **40**, 501–507 (2002)
68. Cheeseman J.M. Hydrogen peroxide concentrations in leaves under natural conditions. J. Exp. Bot. **57**, 2435–2444 (2006).
69. Aebi, H. Catalase in vitro. Methods Enzymol. 105, 121–126 (1984)
70. Nakano, Y., Asada, K. Hydrogen peroxide is scavenged by ascorbate-specific peroxidase in spinach chloroplasts. Plant Cell Physiol. **22**, 867–880 (1981).
71. Macadam, J.W., Nelson, C.J., Sharp, R.E. Peroxidase activity in the leaf elongation zone of tall fescue: I. spatial distribution of Ionically bound peroxidase activity in genotypes differing in length of the elongation zone. Plant Physiol. **99**, 872–878 (1992).

Figures

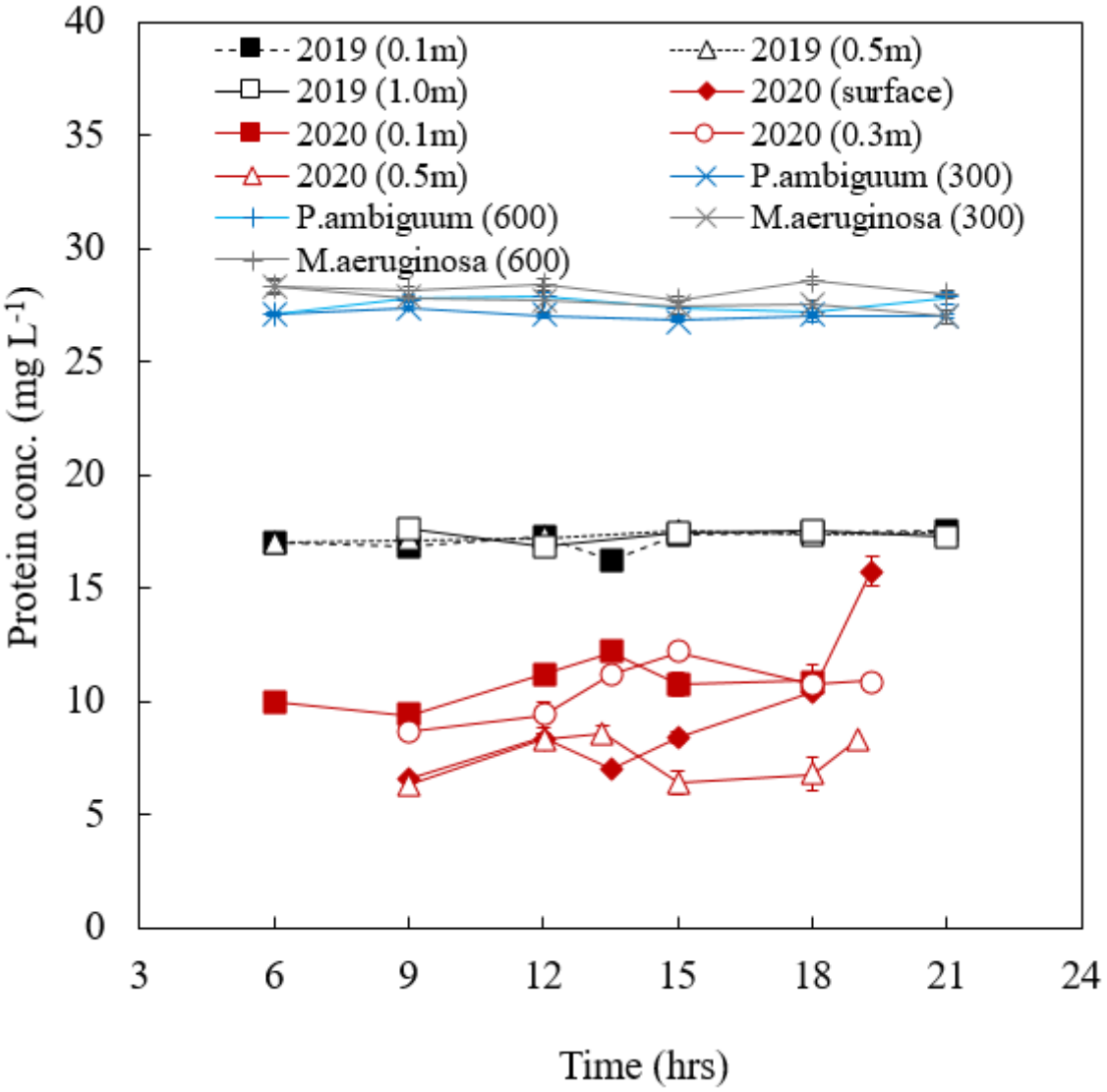

Figure 1

Temporal variation of the total protein content in water

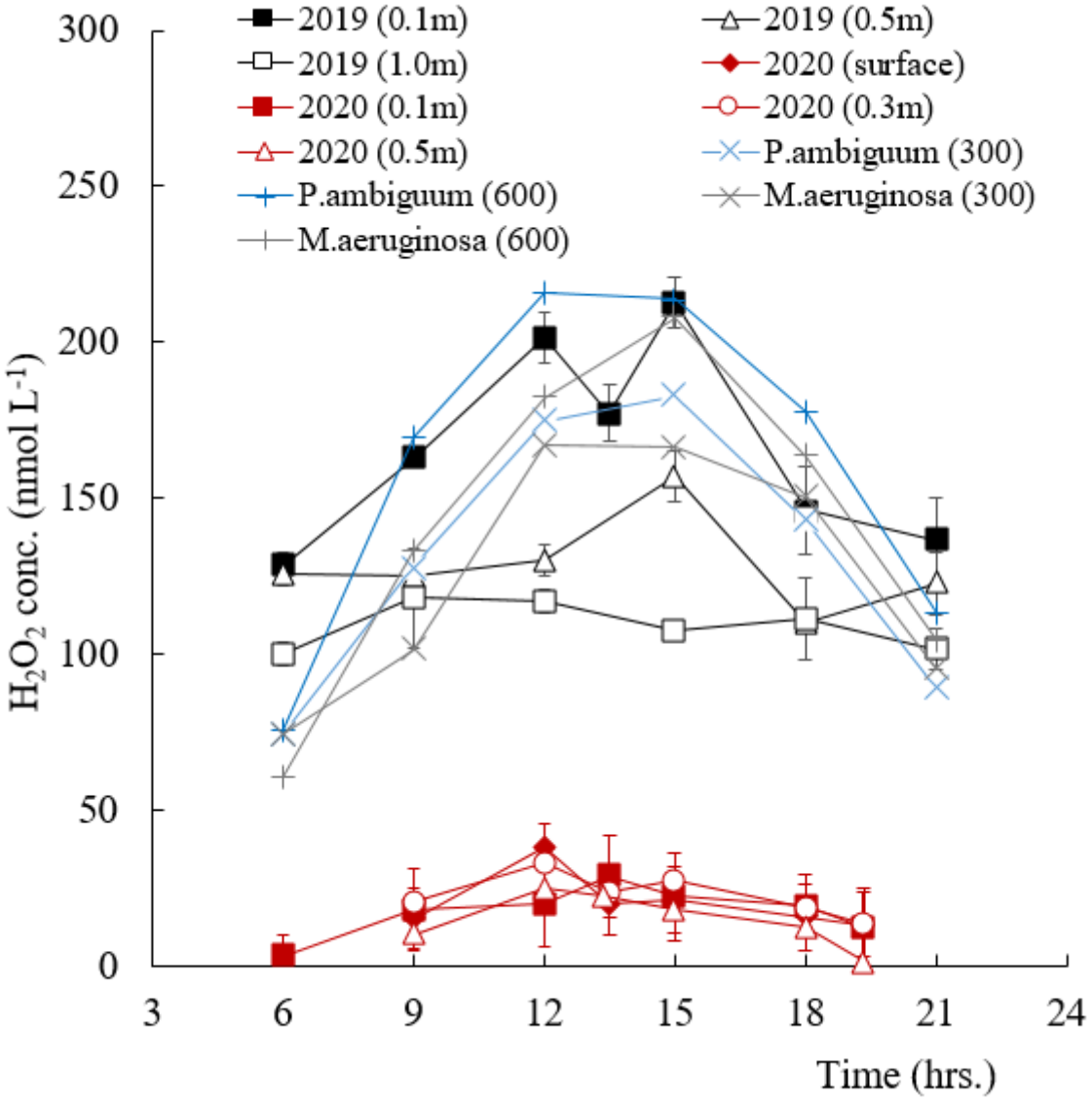

Figure 2

Diurnal variation in H_2O_2 concentration

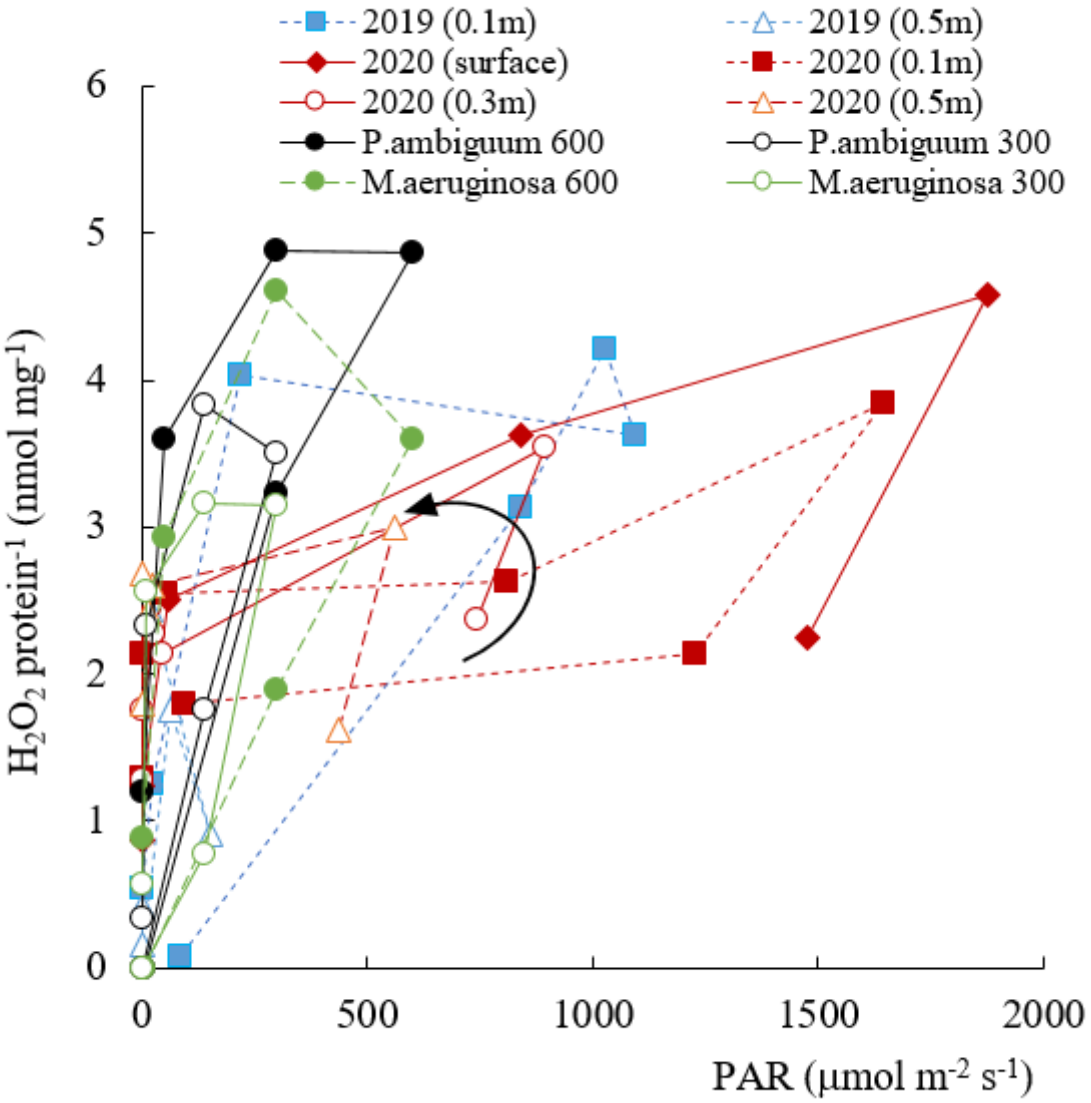

Figure 3

H_2O_2 production per protein in the field and the laboratory experiments against the PAR intensity.

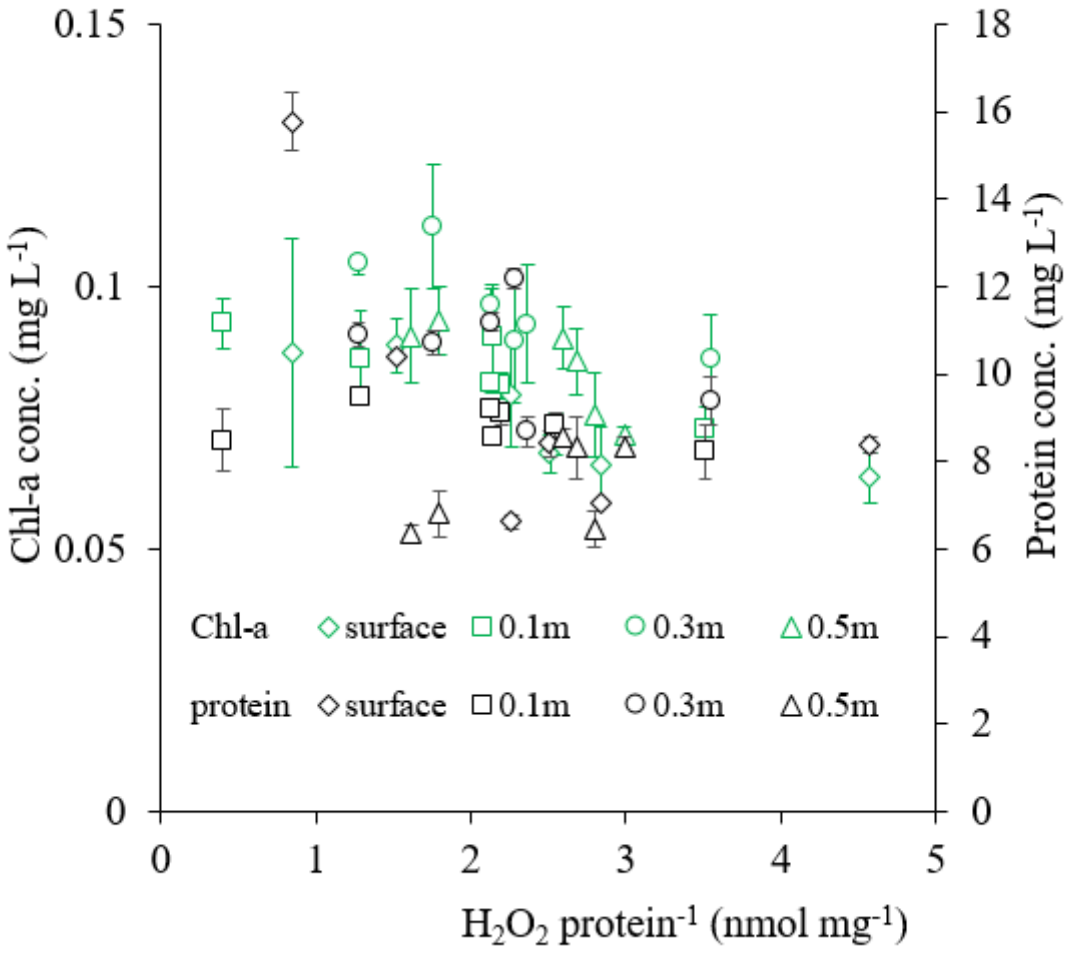

Figure 4

Chl-a and protein contents at different depths as a function of the produced H_2O_2 per protein in 2020 observation.

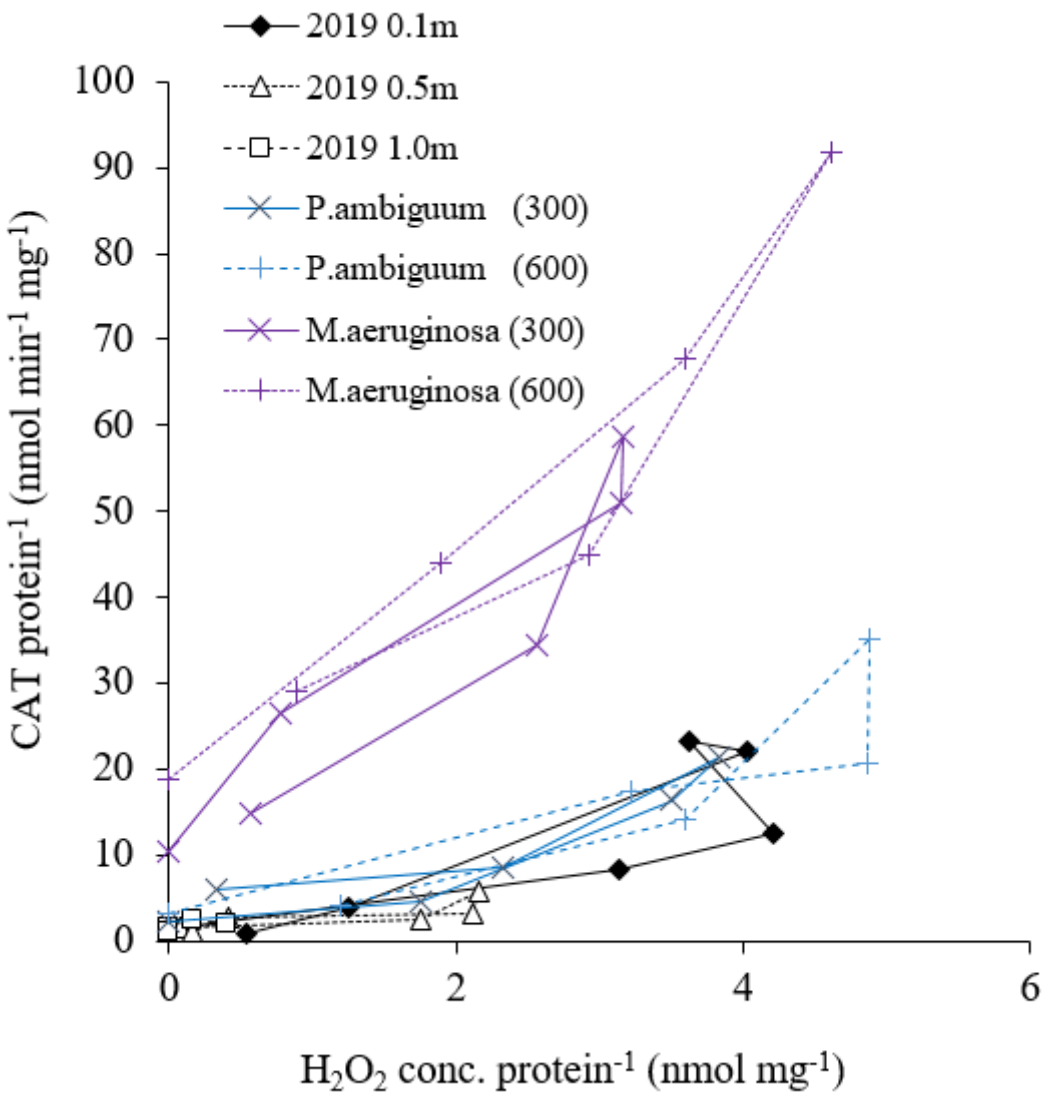

Figure 5

Relationship between the produced H_2O_2 concentration and CAT activity per protein.

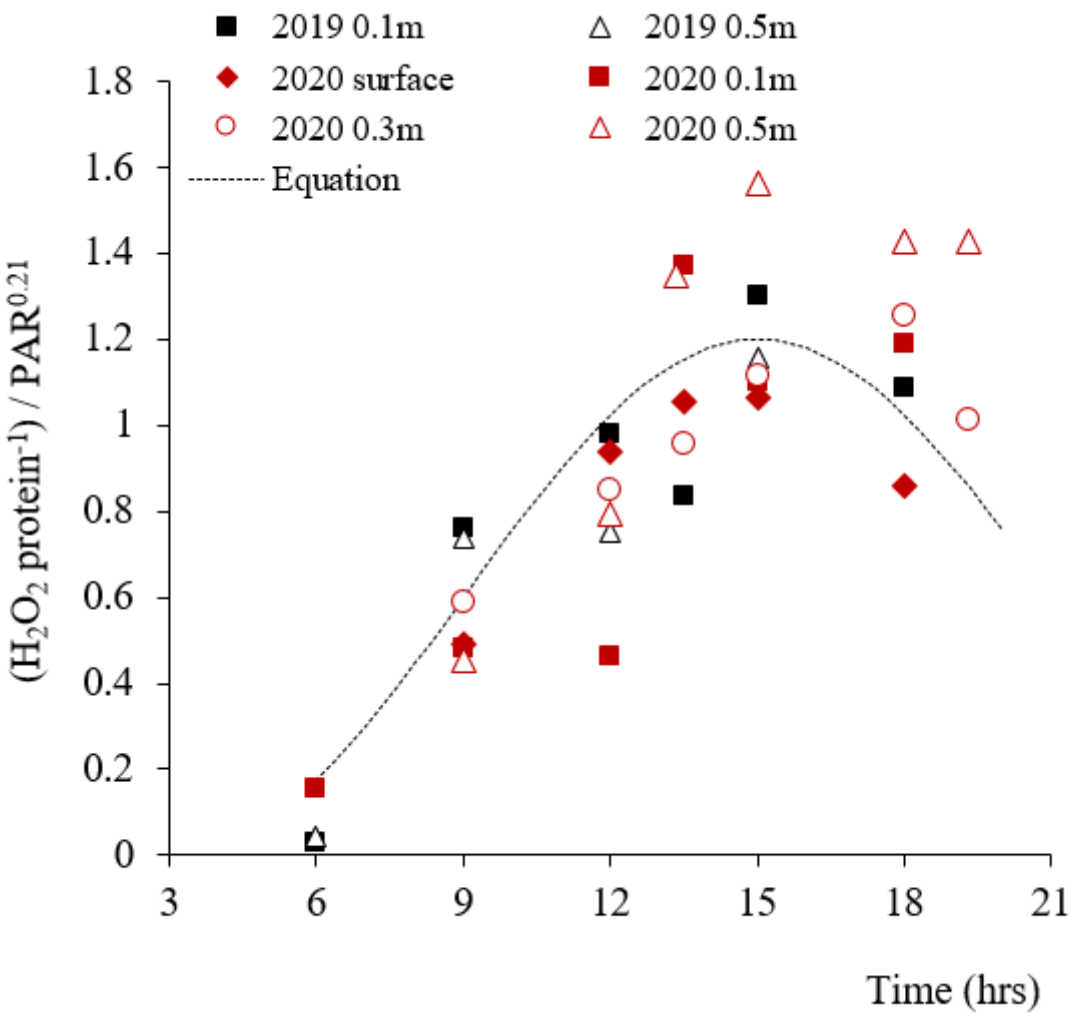

Figure 6

The produced H_2O_2 per protein normalized by $PAR^{0.21}$ as a function of the period from 6:00.

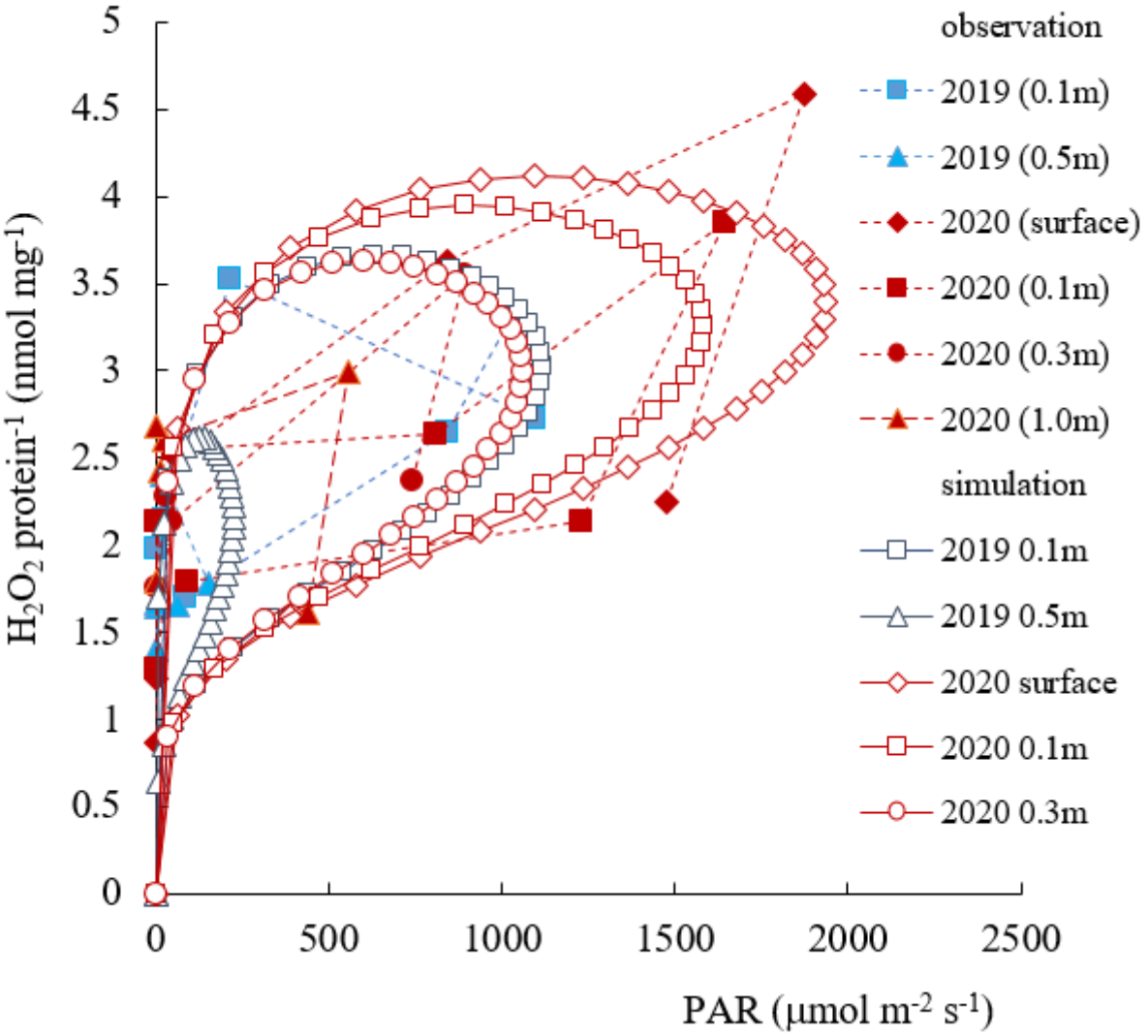

Figure 7

Simulate results of H_2O_2/protein for 2019 and 2020 observations.

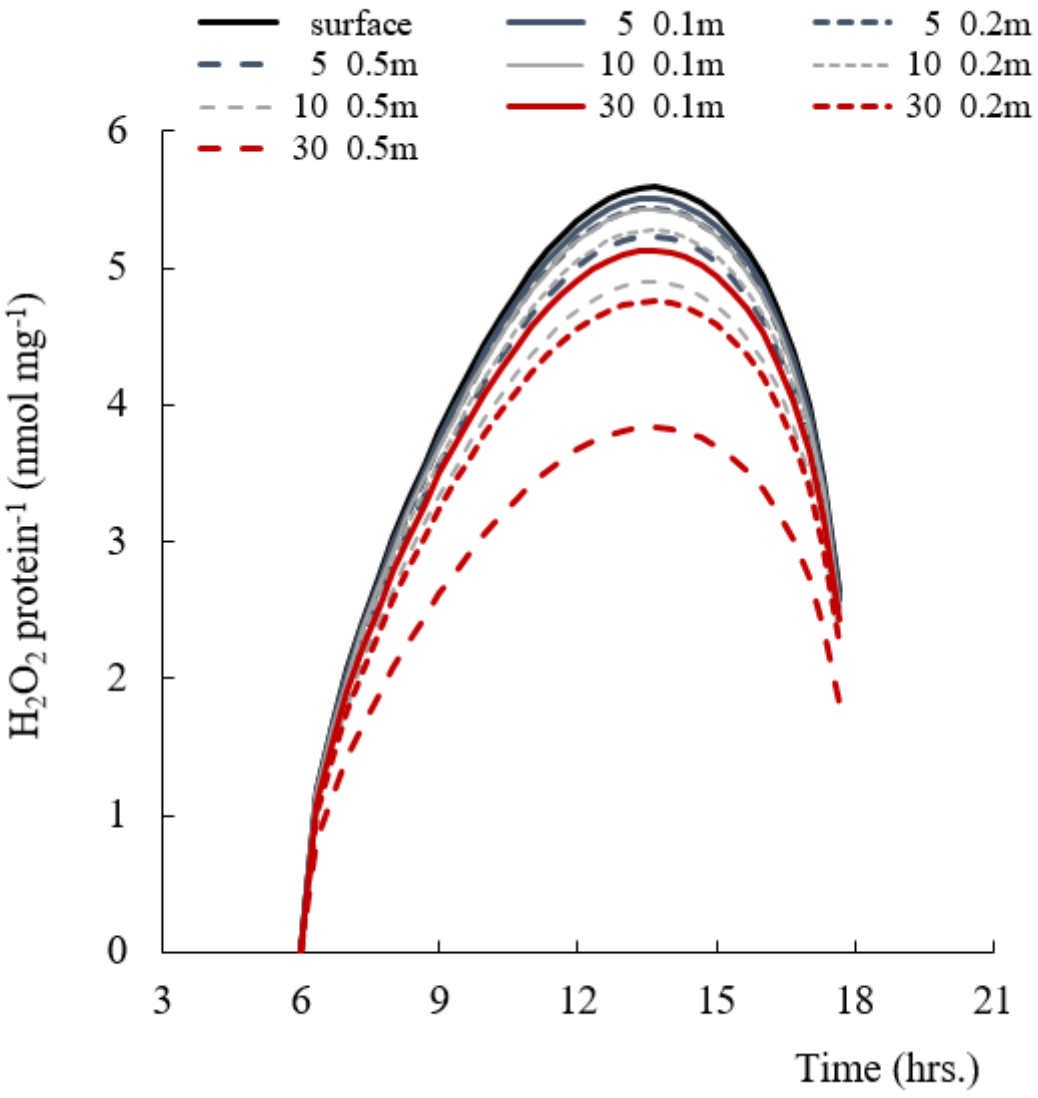

Figure 8

Simulated H2O2 per protein as a function of biomass (protein content) and the mixed layer thickness.

Figure 9

Chidorigafuchi moat at the Imperial Palace, Japan.

Supplementary Files

This is a list of supplementary files associated with this preprint. Click to download.

- Rawdata.docx